

# **In Silico Analysis and Characterization of Differentially Expressed Genes to Distinguish Glioma Stem Cells from Normal Neural Stem Cells**

## **Abstract:**

The main goal of the current study was directed to analyzation and characterization of Differentially Expressed Genes for distinguish Glioma Stem Cells (GSCs) from Normal Neural Stem Cells (NSCs). So, RNA-Seq analysis on NSCs and GSCs samples were used for learning of the differences in their gene expression profiles, as well as about the origins of glioblastomas (GBMs), and to be found potential biomarkers that could be used to selectively target CSCs while sparing normal NSCs via precise medical goals. To identify differences in gene expression, RNA-Seq was used between glioma stem cells and normal neural stem cells. Our research data showed novel genes and genes with no known association with gliomagenesis. Further investigations on the outlier (SRR9200898 PE) would almost certainly reveal important clues to the etiology of this fatal cancer.

**Keywords:** GBM, Glioma Stem Cells, Normal Neural Stem Cells, In Silico

## **Introduction:**

Glioblastomas (GBMs) are primary brain tumors that could arise from oligodendrocyte precursor cells, neural stem cells (NSCs) or astrocytes derived from NSCs. With an incidence rate of 3.21 cases per 100,000 people, a median survival rate of 12-18 months, and a higher male predominance, they are the most lethal and common malignant disorders among all brain tumors. GBMs are also the most commonly diagnosed in elderly patients (median age 65), and their prevalence rises with age, peaking between 75 and 84 years old, but declining after 85 (1-3).

Both genetic and epigenetic mutations are acquired by glioma stem cells (GSCs). Epigenetic changes, similarly to genetic changes, act as catalysts for transformation or work in tandem with genetic events. In contrast to genetic changes, epigenetic changes are theoretically reversible,

which makes them appealing therapeutic targets. DNA methylation (5mC, mediated by the DNA methyltransferases DNMT1, 3A, and 3B) and DNA hydroxymethylation (5hmC, mediated by the ten-eleven translocation complex) are two different types of DNA methylation (4, 5). The TET1, 2 and 3 families are heavily disrupted in GBMs. The prognosis for GBMs patients with G-CIMP (glioma-CpG island hypermethylator phenotype, induced by IDH1/2 mutation) or overall increased 5mC and/or 5hmC levels is better. Although DNA methylation and transcriptional changes in GBMs have been extensively studied, little is known about the epigenetic reprogramming processes that contribute to and/or characterize glioma stem cells, particularly in terms of TET-regulated DNA marks and their relationship to enhancers' activity (6-8).

In the present study, we looked at In Silico Analysis and Characterization of Differentially Expressed Genes to differentiate Glioma Stem Cells from Normal Neural Stem Cells. The researchers utilized RNA-Seq to investigate the differences in gene expression patterns between NSCs and GSCs.

## **Methods:**

- **Acquisition of RNA-Seq Data**

To find the perfect dataset for the study, a thorough search of the Gene Expression Omnibus (GEO) Database was conducted. The SRP200400 related Sequence Retrieval Archive (SRA) Study dataset GSE132172 was selected (9). Twenty samples of NSCs (SRR9200813 to SRR9200832) and 20 samples of GSCs (SRR9200895 to SRR9200914) were chosen from the 188 samples on the associated SRA Run Selector and downloaded as an SRA.

- **RNA-Seq Data Analysis**

The PCR clean and Trimmomatic methods were used to remove adaptor sequences and low-quality sequencing data. The genome and junctions were mapped using TopHat2; to build isoforms, Cufflinks was utilized; Cuffmerge was used to process GTFs; Bowtie2-t was used to map transcripts; and the final gene expression levels were produced using the RSEM method as

RsemExpTable in Fragments Per Kilobase o For further analysis, the gene expression data was log transformed and quantile normalized.

- **Downstream Data Analysis**

The 40 samples were classified using Principal Component Analysis and Hierarchical Clustering based on their gene expression patterns (distance: Euclidean, linkage: ward.D2). Using differential gene expression, the DESeq2 pipeline was utilized to identify highly expressed genes in GSCs and NSCs samples. The differential gene expression data was filtered and retrieved if the threshold = TRUE, the p-adjusted value was 0.05, and the log2fold change value for GSCs was 3.0 (for GSCs) and -3.0 (for GSCs) (for NSCs). The top 25 most highly expressed genes in each kind of stem cell sample were further filtered, and a heat map and dendrogram were produced to analyze gene expression patterns across samples.

- **Gene Enrichment Analysis**

The gene lists were uploaded to the Database for Annotation, Visualization, and Integrated Discovery (DAVID) v6.8 software to investigate the biological implications of the significant genes discovered via differential gene expression analysis. For pathway analysis, the Kyoto Encyclopedia of Genes and Genomes (KEGG) was used. Researchers searched Google Scholar, National Center for Biotechnology Information (NCBI) PubMed, and GeneCards® for the top 50 most significant differentially expressed genes in normal physiological circumstances and during gliomagenesis to better understand their roles (which included the top 25 upregulated and top 25 downregulated genes in GSCs vs. NSCs).

## **Results and Discussion:**

After running the RNA-Seq Pipeline, the RsemExp table included gene expression data in FPKM units for a total of 27,385 genes (Tuxedo Protocol). PCA plots showed different clustering of GSCs and NSCs data after quantile normalization and logscale transformation, with a principal component 1 (PC1) of 10.31 percent and a principal component 2 (PC2) of 8.9 percent. 1a (extra figure) A single outlier, a glioma stem cell sample (SRR9200898 PE), was

discovered. As a result, a new PCA plot was created without the outlier. This plot yielded a PC1 of 88.03 percent and a PC2 of 2.13 percent (supplementary figure 1b). Hierarchical clustering was used to confirm these findings, and it revealed that NSCs samples (SRR9200813 to SRR9200832) and GSCs samples (SRR9200895 to SRR9200897 and SRR9200899 to SRR9200914), clustered separately.

Between the two clusters, the outlier GSCs sample (SRR9200898 PE) was sandwiched (supplementary figure 2).

Differential gene expression analysis found 12,437 differently expressed genes between the NSCs and GSCs samples (45.42 percent of the total genes). To illustrate the significant differences in gene expression between NSCs and GSCs, a volcano graphic was created (figure 3). The genes that varied the most between NSCs and GSCs were filtered once more to find the genes that differed the most. For the log2fold change value, a threshold of 3.0 (for GSCs) and -3.0 (for NSCs) was set. As a consequence, 348 genes had substantially varied levels of expression. We also chose the top 50 significantly different expressed genes in GSCs vs. NSCs, as well as the top 25 upregulated genes and downregulated genes (Table 1).

**Table 1: Top 50 genes that vary in expression between GSCs and NSCs**

Downregulated Genes			Upregulated Genes		
ENSEMBL Gene ID	Entrez Gene ID	Log <sub>2</sub> fold change	ENSEMBL Gene ID	Entrez Gene ID	Log <sub>2</sub> fold change
ENSG00000163191.5	S100A11	-5.437646	ENSG00000160307.8	S100A11	-5.437646
ENSG00000170315.12	UBB	-5.334275	ENSG00000197956.8	UBB	-5.334275

XLOC_02925 2	unknown	-5.0073837	ENSG000001 89 058.7	Unknown	-5.0073837
ENSG000000 08394.11	MGST1	-4.9702519	ENSG000001 35 919.11	MGST1	-4.9702519
ENSG000001 32386.9	SERPINF1	-4.9191335	ENSG000002 61 857.5	SERPINF1	-4.9191335
ENSG000001 52583.11	SPARCL1	-4.8928578	ENSG000002 29 344.1	SPARCL1	-4.8928578
ENSG000001 97614.9	MFAP5	-4.8696255	ENSG000001 36 235.14	MFAP5	-4.8696255
ENSG000002 13145.8	CRIP1	-4.8111644	ENSG000001 23 560.12	CRIP1	-4.8111644
ENSG000001 39329.4	LUM	-4.7388415	ENSG000001 47 588.6	LUM	-4.7388415
ENSG000001 01335.8	MYL9	-4.6796897	ENSG000000 78 596.9	MYL9	-4.6796897
ENSG000001 09113.16	RAB34	-4.6787092	ENSG000001 54 096.12	RAB34	-4.6787092

ENSG000001 98467.12	TPM2	-4.6243914	ENSG000001 60 862.11	TPM2	-4.6243914
ENSG000001 28610.10	FEZF1	-4.5842385	ENSG000001 29 824.14	FEZF1	-4.5842385
ENSG000001 38829.9	FBN2	-4.5675219	ENSG000001 10 693.14	FBN2	-4.5675219
ENSG000002 25383.5	SFTA1P	-4.5507508	ENSG000001 64 434.10	SFTA1P	-4.5507508
ENSG000001 31435.11	PDLIM4	-4.5340762	ENSG000001 54 553.12	PDLIM4	-4.5340762
ENSG000001 04723.19	TUSC3	-4.4994617	ENSG000001 64 106.6	TUSC3	-4.4994617
ENSG000001 29038.14	LOXL1	-4.4942203	ENSG000001 32 561.12	LOXL1	-4.4942203
ENSG000000 67715.12	SYT1	-4.4821866	ENSG000001 23 610.4	SYT1	-4.4821866
ENSG000001 05971.13	CAV2	-4.4721796	ENSG000000 07 237.17	CAV2	-4.4721796

ENSG000001 37962.11	ARHGAP2 9	-4.4720021	ENSG000002 55 737.2	ARHGAP2 9	-4.4720021
ENSG000001 27083.7	OMD	-4.4647095	ENSG000002 40 747.6	OMD	-4.4647095
XLOC_01200 3	Pro-neural	-4.4462352	ENSG000001 84 221.11	Pro-neural	-4.4462352
ENSG000001 46411.5	SLC2A12	-4.4290885	ENSG000002 41 990.4	SLC2A12	-4.4290885
XLOC_04736 7	p53- regulated lncRNAs	-4.4287433	ENSG000001 36 999.4	p53- regulated lncRNAs	-4.4287433

Next, we created PCA plots with only these significant genes with the outlier (Figure 1a) and without the outlier (Figure 1b) to determine the distinguishable potential of these top 50 significantly differentially expressed genes (Figure 1b). The differential expression pattern of these genes was then visualized in the heatmap (Figure 2) between two types of samples, i. e., GSCs vs NSCs.

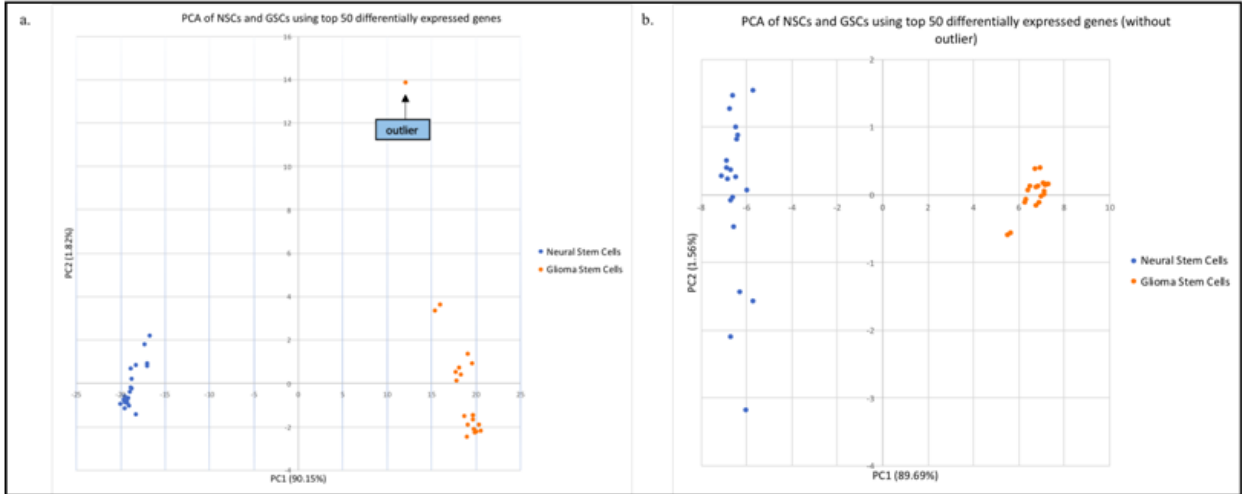


**Figure 1: Exploratory data analysis using PCA based on the top 50 significantly differentially expressed genes between NSCs and GSCs. (a). PCA plot for all GSC and NSC samples, (b) PCA plot for GSC and NSC samples after removal of outlier**

UNDER PEER REVIEW

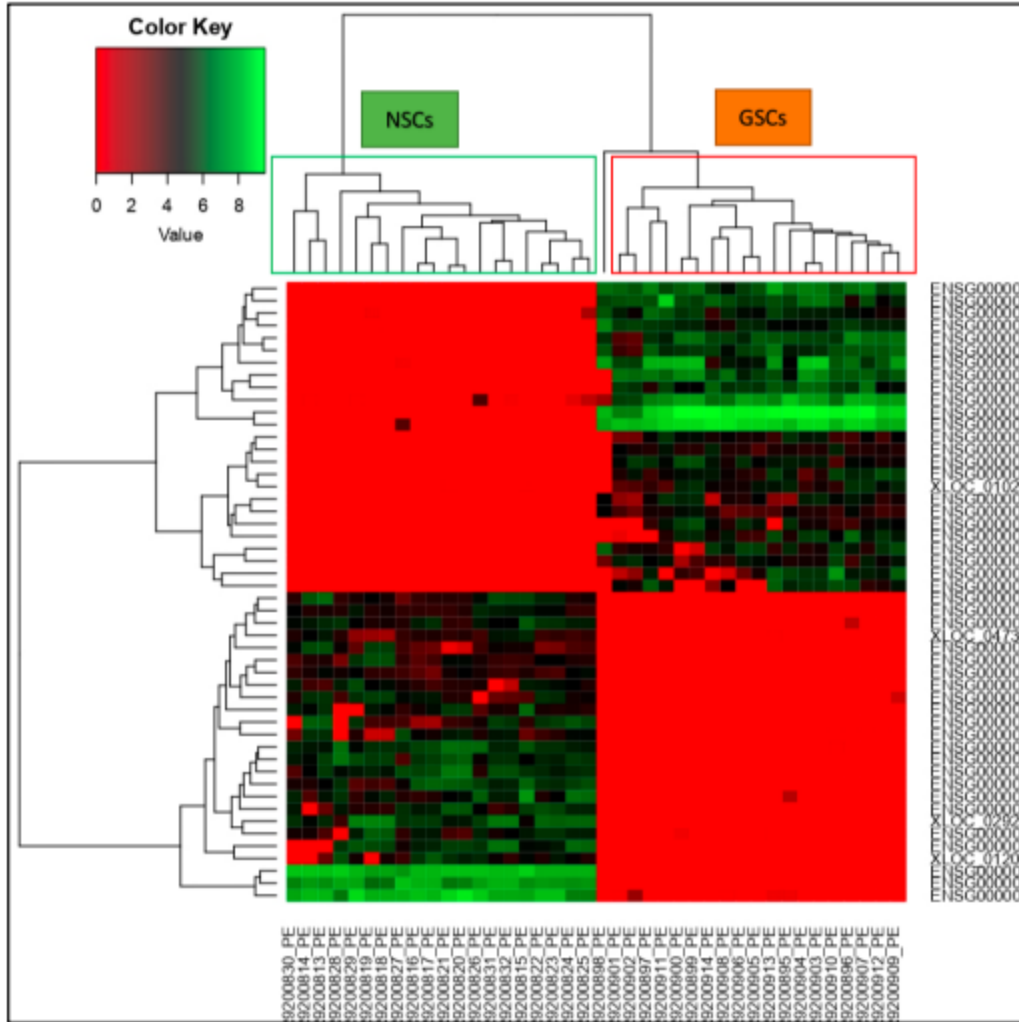


**Figure 2: Heat map representing the expression pattern of the top 50 differentially expressed genes expressed genes between NSCs and GSCs.**

Finally, we ran H-Clustering again using the top 50 genes (Figure 3). The GSCs and NSCs samples clustered independently, with the outlier sample branching in between.

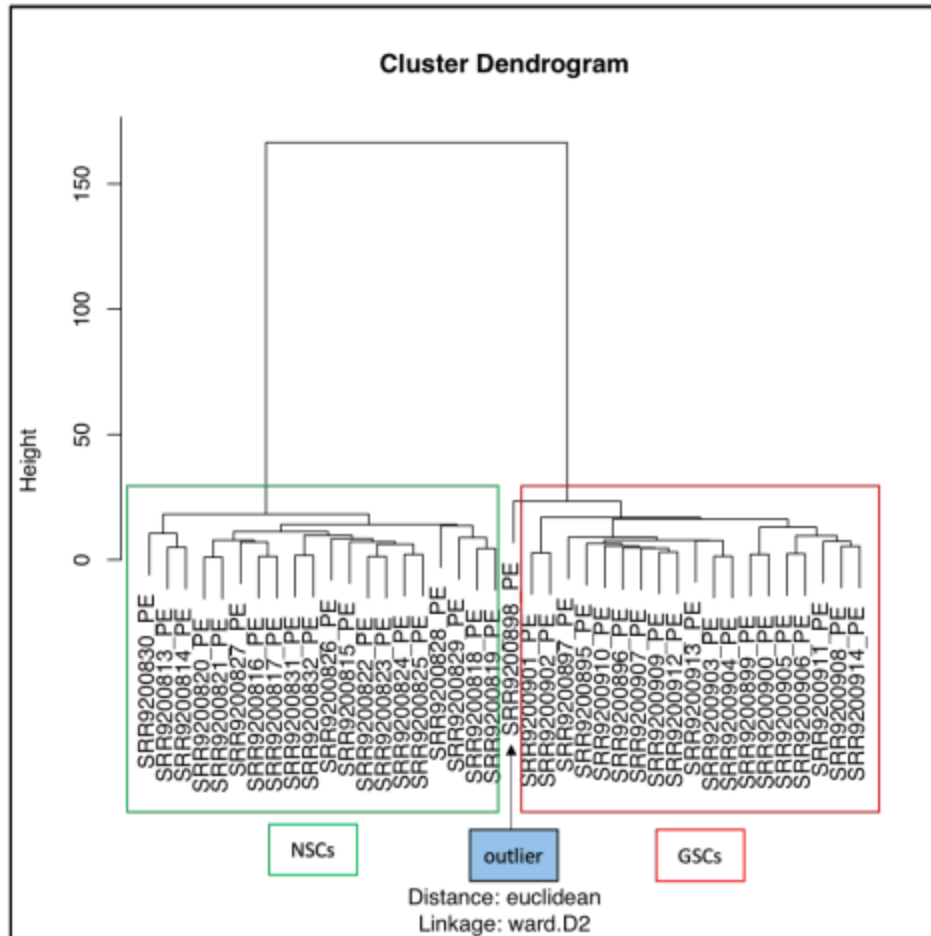


**Figure 3: The unique groups of GSCs and NSCs samples are shown in a dendrogram produced by hierarchical clustering based on the top 50 substantially differentially expressed genes**

### Gene Enrichment analysis

On DAVID, the gene list for NSCs (156 genes) and GSCs (192 genes) was uploaded, and functional annotation and clustering were performed. *Alzheimer's* disease, respiratory function tests, Tobacco Use Disorder, body weight, bone mineral density, macular degeneration, alcoholism, and other diseases were among the top hits with the NSCs gene list. Extracellular matrix, secreted, glycoprotein, signal, calcium, disulphide bond, disease mutation, membrane, and transmembrane were among the top keyword annotations. Signal peptide, N-linked glycosylation, Leucine Rich Repeats (LRR 6), EGF-like 6, LRR 5, LRR 1, LRR 2, LRR 7, LRR 4, disulphide bond, and topological domain were among the top sequence features found

(cytoplasmic). Functional clustering (medium stringency) revealed 27 clusters with 137 DAVID IDs, with the top three clusters involved in extracellular matrix, glycoprotein, and LRRs, respectively, and enrichment scores of 5.99, 4.95, and 2.05. Schizophrenia, Attention deficit hyperactivity disorder (ADHD), tobacco use disorder, depression, body height, body weight, autism, and myocardial infarction were among the top diseases found in the GSC gene list, which contained 192 genes. Disulphide bond, glycoprotein, signal, MHC-II, cell adhesion, cell membrane, alternative splicing, polymorphism, and transmembrane were among the top keyword annotations. Glycosylation (N-linked), signal peptide, disulphide bond, topological domain (extracellular and cytoplasmic), transmembrane, splice variant, and sequence variant were among the top hits for sequence features. The top three clusters were involved in glycoprotein disulphide bonds, melanocyte differentiation metallo-thionein domain, and had enrichment scores of 6.17, 2.35, and 2.15, respectively, according to functional clustering (medium stringency).

Ankyrin, 21, Lumican, Wnt, 51, SDC-4, and Caveolin were identified as being involved in various tumorigenesis pathways by KEGG Pathway analysis. PVRL3, PVRL2, NCAM, L1CAM, IGSF4, CDH3, and NEO1, which are enriched in the nervous system, were also shown. In the pathway analysis, ECM Receptor Interaction genes such as Fibronectin, Collagen, Laminin, Tenascin, V, 8, Thrombospondin (THBS) and Osteopontin (OPN), were found. Genes involved in axon guidance pathways, such as FAK, PAK, RasGAP, Ephrin A, Ephrin B, Robo1, Robo3, ERK, Cofilin, GSK3, Plexin B, and genes involved in calcium signaling pathways, such as PLC, PLC, RTK and PMCA, were also enriched in the gene lists (Figure 4).

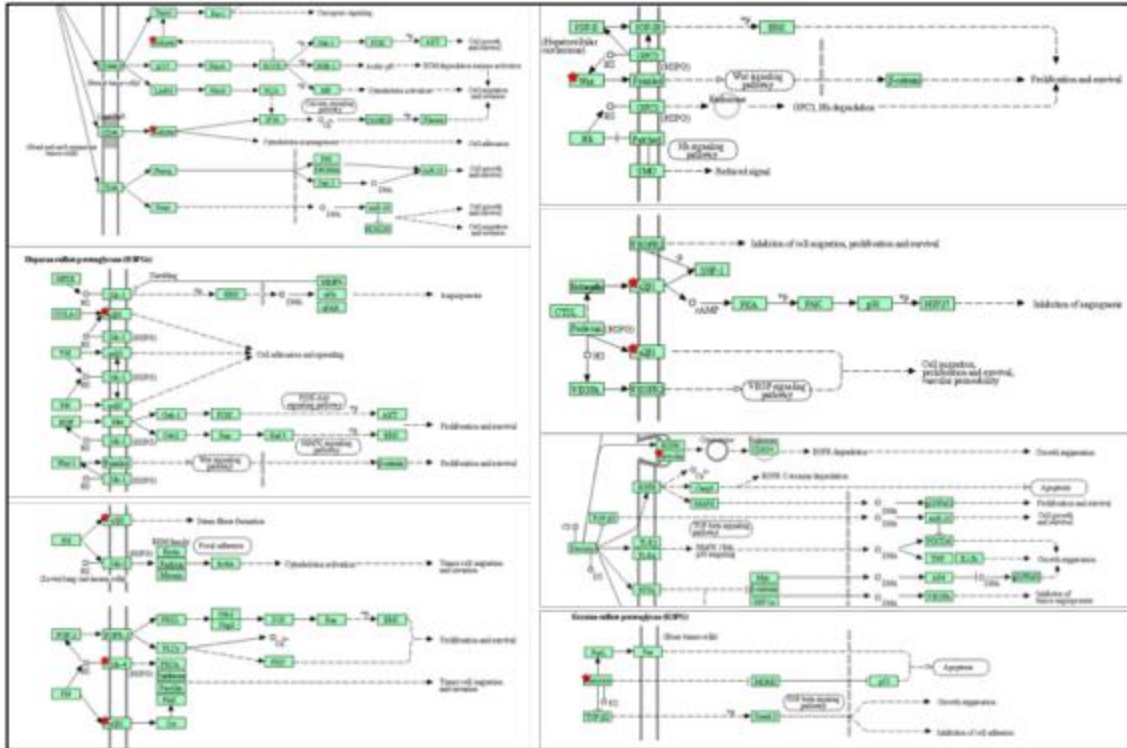


**Figure 4: Pathway analysis of significant genes in GSC and NSC samples**

The top 25 highly upregulated and 25 highly downregulated genes in GSCs and NSCs, as well as their roles and functions in normal pathophysiology and gliomagenesis, are tabulated in Tables (see Supplementary tables S1 and S2). Upregulated genes like S100B, S100A6, GPNMB, CD90, and SOX10, to name a few, have been linked to gliomagenesis, whereas genes like ITM2A, KRBOX1, PRR34-AS1, SLCO4A1, and the novel gene ENSG00000154553 have not been linked to the disease (10). S100A11, UBB, MGST1, SERPINF1, and SPARCL1 are similarly downregulated genes with established associations, whereas no previous association has been established for XLOC 02 9252 (novel gene), FBN2, SFTA1P, OMD, XLOC 01 2003 (novel gene), XLOC 04 7367 (novel gene) (11).

### Conclusion:

The epigenetic changes, similarly to the genetic changes, act as catalysts for transformation or work in tandem with genetic events. In contrast to genetic changes, epigenetic changes are

theoretically reversible, which makes them appealing therapeutic targets. Glycosylation (N-linked), signal peptide, disulphide bond, topological domain (extracellular and cytoplasmic), transmembrane, splice variant and sequence variant, were among the top hits for sequence features. The top three clusters were involved in glycoprotein disulphide bonds, melanocyte differentiation metallothionein domain, and had enrichment scores of 6.17, 2.35 and 2.15, respectively, according to functional clustering (medium stringency).

## References:

1. Patel AP, Tirosh I, Trombetta JJ, Shalek AK, Gillespie SM, Wakimoto H, et al. Single-cell RNA-seq highlights intratumoral heterogeneity in primary glioblastoma. *Science*. 2014; 344: 1396–1401. doi: 10.1126/science.1254257
2. Towner, R. A. et al. Experimental validation of 5 in-silico predicted glioma biomarkers. *Neuro Oncol*. 2013; 15: 1625–1634.
3. Louis DN, Perry A, Reifenberger G, von Deimling A, Figarella-Branger D, Cavenee WK, et al. The 2016 World Health Organization Classification of Tumors of the Central Nervous System: a summary. *Acta Neuropathol* 2016; 131: 803–820, doi: 10.1007/s00401-016-1545-1.
4. Gamazon ER, Stranger BE. The impact of human copy number variation on gene expression. *Brief Funct Genomics* 2015; 14: 352–357, doi: 10.1093/bfgp/elv017.
5. Veeriah S, Brennan C, Meng S, Singh B, Fagin JA, Solit DB, et al. The tyrosine phosphatase PTPRD is a tumor suppressor that is frequently inactivated and mutated in glioblastoma and other human cancers. *Proc Natl Acad Sci USA* 2009; 106: 9435–9440, doi: 10.1073/pnas.0900571106.
6. Mukherjee, S. (2020). Quiescent stem cell marker genes in glioma gene networks are sufficient to distinguish between normal and glioblastoma (GBM) samples. *Scientific Reports*, 10(1), 1-18.
7. Gagliardi, F., Narayanan, A., Gallotti, A. L., Pieri, V., Mazzoleni, S., Cominelli, M., & Galli, R. (2020). Enhanced SPARCL1 expression in cancer stem cells improves

preclinical modeling of glioblastoma by promoting both tumor infiltration and angiogenesis. *Neurobiology of disease*, 134, 104705.

8. Ramaswamy, V.; Remke, M.; Bouffet, E.; Bailey, S.; Clifford, S.C.; Doz, F.; Kool, M.; Dufour, C.; Vassal, G.; Milde, T.; et al. Risk stratification of childhood medulloblastoma in the molecular era: The current consensus. *Acta Neuropathol.* 2016, 131, 821–831.
9. Zhao, Y., Carter, R., Natarajan, S., Varn, F.S., Compton, D.A., Gawad, C., Cheng, C., Godek, K.M., 2019. Single-cell RNA sequencing reveals the impact of chromosomal instability on glioblastoma cancer stem cells. *BMC Med. Genomics* 12, 79. <https://doi.org/10.1186/s12920-019-0532-5>.
10. Azimi, I.; Milevskiy, M.J.G.; Chalmers, S.B.; Yapa, K.T.D.S.; Robitaille, M.; Henry, C.; Baillie, G.J.; Thompson, E.W.; RobertsThomson, S.J.; Monteith, G.R. ORAI1 and ORAI3 in Breast Cancer Molecular Subtypes and the Identification of ORAI3 as a Hypoxia Sensitive Gene and a Regulator of Hypoxia Responses. *Cancers* 2019, 11, 208.
11. Brandalise, F.; Ratto, D.; Leone, R.; Olivero, F.; Roda, E.; Locatelli, C.A.; Grazia Bottone, M.; Rossi, P. Deeper and Deeper on the Role of BK and Kir4.1 Channels in Glioblastoma Invasiveness: A Novel Summative Mechanism? *Front. Neurosci.* 2020, 14, 1237.